Int. J. Heat Mass Transfer. Vol. 23, pp. 677–686.
Pergamon Press Ltd. 1980. Printed in Great Britain

NATURAL CONVECTION IN A SHALLOW ANNULAR CAVITY

G. P. MERKER*

Lehrstuhl A für Thermodynamik, Technische Universität München, West Germany

L. G. LEAL

Department of Chemical Engineering, California Institute of Technology, Pasadena, CA, U.S.A.

(*Received* 13 *March* 1979 *and in revised form* 4 *September* 1979)

Abstract — The problem of natural convection in a shallow annular cavity with differentially heated inner and outer walls is considered. Compared to the two-dimensional problem Cormack, Leal and Imberger[3], the flow structure differs in two important ways. First the core flow is only parallel at $O(1)$ in the annulus. Second, the finite radius of the inner cylinder provides a third length scale in addition to h and $(r_c - r_h)$. Therefore, the flow consists of two distinct regimes in the asymptotic limit, $A = h/(r_c - r_h) \to 0$. The solution in the core is developed correct to $O(A^2)$, and asymptotic results are then obtained for the Nusselt number, valid to $O(A^3)$.

NOMENCLATURE

A,	cavity aspect ratio, $= h/(r_c - r_h)$;
A_n,	end solution coefficients;
c_i,	coefficients which are functions of Gr and Pr;
c_p,	heat capacity;
$f_i(\hat{x};\rho)$,	core solutions;
$F(z)$,	power function for core solution, equation (28a);
$F_n(x)$,	power function for end solution;
g,	gravitational acceleration constant;
$g_i(\hat{x};\rho)$,	core solutions;
$G(z)$,	power function for core solution, equation (28b);
Gr,	Grashof number, $= gh^3\beta(T_h - T_c)/v^2$;
h,	cavity height;
$h_i(\hat{x};\rho)$,	core solutions;
$H(z)$,	power function for core solution, equation (28c);
$J(A,B)$,	Jacobian, $= \dfrac{\partial A}{\partial x}\dfrac{\partial B}{\partial z} - \dfrac{\partial B}{\partial x}\dfrac{\partial A}{\partial z}$;
k,	thermal conductivity;
$k_i(\hat{x};\rho)$,	core solutions;
l,	cavity length, $= r_c - r_h$;
$m_i(\hat{x};\rho)$, $n_i(\hat{x};\rho)$,	core solutions;
Nu,	Nusselt number, $= \dot{Q}/2\pi\lambda r_h(T_h - T_c)$;
Pr,	Prandtl number, $= c_p\mu/k$;
$\dot{Q}$,	heat flux;
r_c, r_h,	cold- and hot-end wall radii;
T_c, T_h,	cold- and hot-end wall temperatures;
u, w,	horizontal and vertical velocity components;
x, z,	horizontal and vertical coordinates non-dimensionalized by h;
$\hat{x}$,	horizontal coordinate in the core, $= Ax$.

*Since 1 April 1978 with MTU-München GmbH, P.O. Box 50 06 40, 8000 Munich 50, West Germany.

Greek symbols

β,	coefficient of thermal expansion;
δ,	length scale ratio, $= r_h/h$;
θ,	non-dimensional temperature, $= (T - T_c)/(T_h - T_c)$;
λ,	thermal conductivity;
μ,	dynamic viscosity;
v,	kinematic viscosity;
∇_2^2,	two-dimensional Laplace operator, $= \dfrac{\partial^2}{\partial x^2} + \dfrac{\partial^2}{\partial z^2}$;
ξ,	horizontal distance from hot end of cavity, $= A^{-1} - x$;
ρ,	annulus aspect ratio, $= A\delta$;
ω,	vorticity;
ψ,	stream function.

Superscripts

$\hat{}$,	perturbated quantity;
$\bar{}$,	basic state;
c,	cold;
h,	hot;
i,	order of approximation, $i = 0, 1, 2\ldots$

Subscripts

c,	cold;
h,	hot;
i,	order of approximation, $i = 0, 1, 2\ldots$

1. INTRODUCTION

THE PROBLEM of gravitational convection in a shallow, two-dimensional cavity with a temperature differential maintained between the side-walls has been studied recently by several authors because of its potential as a model for certain aspects of atmospheric circulation (Hadley cells; cf. Hart[1]); and for the dispersion of pollutants or heat wastes in estuary or other shallow bodies of water (cf. Cormack, Stone and Leal[2]). In particular, Hart[1] examined the stability of the basic, unidirectional flow which occurs in the central domain when the top and bottom of the cavity are insulated. At nearly the same time, Cormack, Leal and Imberger[3] showed that an asymptotically rigorous solution could be obtained (also for insulated top and bottom) by using the height-to-width aspect ratio, A, as a small parameter for arbitrary but fixed values of the Grashof and Prandtl numbers, Gr and Pr. This solution consisted of a 'core' flow over the interior of the cavity, which was matched in the usual asymptotic sense with solutions in the regions within $O(h)$ of the side-walls. Here, h denotes the height of the cell. The unusual feature of the solution, which was qualitatively verified both by experiment[4] and by numerical solution of the full governing equations (Cormack, Leal and Seinfeld[5]), was that the flow in the core remained parallel and unidirectional to all orders in the small parameter A. Although it seemed clear that this result was a direct consequence of the two-dimensional geometry and of the simple insulating boundary conditions, the degree of sensitivity to those conditions was not at all evident nor, more importantly, was the effect of deviations from the parallel flow structure on the efficiency of heat flow away from the heated boundary. The latter, measured in dimensionless terms by the relationship between Nusselt number (heat flux), Grashof number (ΔT) and the other parameters (A, Pr) of the system, is particularly significant due to the obvious relationship between Nu and the effectiveness of pollutant or heat waste dispersion in a shallow estuary.

The effect of the thermal boundary conditions at the top of the cavity was investigated in some detail by Cormack, Stone and Leal[2]. The present communication is concerned with the effects of cavity geometry. In particular, we consider the simplest generalization from the 2-D case of Cormack, Leal and Imberger[3] to a shallow annular cavity with the inner cylinder maintained at a temperature, T_h, and the outer at a lower temperature, T_c. This problem includes the original two-dimensional solution as a limiting case, but differs significantly in flow structure away from this limit. Specifically, we will see that the 'parallel flow' assumption in the core region (i.e. radial flow for this annular geometry) is only adequate at the lowest order approximation. In this sense, the problem of convection in a shallow annular cavity provides a useful model for illustration of the type of effects engendered by flow geometries which are not two-dimensional.

The problem is also of some direct interest on its own as a crude model for the gravitational circulation and efficiency of heat release associated with a source of heat in the center of a lake or estuary. For example, one might imagine hot effluent released at the bottom with negligible momentum. In addition, the annular geometry is sometimes used, with the central cylinder a heated wire, as a 'conduction' cell for determination of thermal conductivities. The present analysis provides an analytical solution for *a priori* estimation of the importance of convection effects at steady state in such a system.

The analysis which follows is similar in many respects to that which was described in detail by Cormack, Leal and Imberger[3]. Thus, wherever possible we present an abbreviated description of the method in the present paper. Unlike Cormack *et al.*[3], we do *not* obtain complete solutions in the end regions but rather concentrate on the core velocity and temperature distributions and on the overall Nusselt number which is obtained through terms of $O(A^3)$. Another difference is the fact that the radius of the inner cylinder provides a third length scale (in addition to the height of the cavity, h, and the separation distance, $r_c - r_h$). Thus, in addition to the aspect ratio, $A \equiv h/(r_c - r_h)$, which we assume to be small, there is a second dimensionless parameter

$$\delta = \frac{r_h}{h}$$

which enters the calculations. Obviously, the combination

$$\rho = A\delta = \frac{r_h}{(r_c - r_h)}$$

defines yet a third length scale ratio. Any two of A, δ and ρ are independent. We consider two distinct problems. In the first $A \to 0$, with $\rho = O(1)$ (and thus $\delta \gg 1$ for $A \ll 1$), while, in the second, $A \to 0$ with $\delta = O(1)$ (and thus $\rho \to 0$ for $A \to 0$). The latter is the more interesting from the point of view of the direct 'applications' which were noted above. However, the former encompasses the 2-D problem as the limiting case of $\delta \to \infty$ (with $A \to 0$). Surprisingly in view of apparent differences in the governing equations and analysis for the two cases, we will see that the core solutions are identical through the first two levels of approximation.

2. MATHEMATICAL FORMULATION OF THE PROBLEM

We consider a closed annular cavity with inner radius r_h, outer radius r_c and height h, as shown schematically in Fig. 1(a). The cavity contains a Newtonian fluid, and the inner and outer walls are held at different but uniform temperatures T_c and T_h with

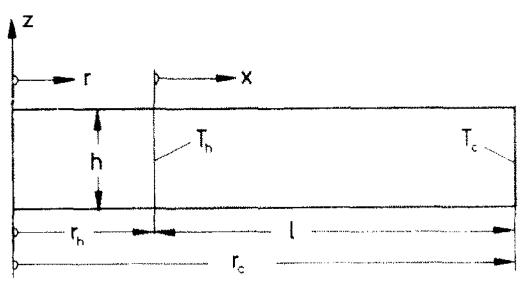

FIG. 1(a). Schematic diagram of system.

$T_h > T_c$. The top and bottom are insulated, and all surfaces are rigid, no-slip boundaries.

The flow which results from heating the inner cylinder is axisymmetric, and the governing differential equations and boundary conditions are easily obtained, subject to the Boussinesq approximation, from the full, steady-state equations of motion and thermal energy expressed in terms of cylindrical coordinates. We denote the horizontal and vertical velocity components by u and w. Thus, nondimensionalizing in the manner of Cormack *et al.*[3] with $l = r_h - r_c$, and introducing a streamfunction

$$u = -\frac{1}{x+\delta}\frac{\partial\psi}{\partial z}, \quad w = \frac{1}{x+\delta}\frac{\partial\psi}{\partial x} \tag{1}$$

the governing equations and boundary conditions can be written in the form

$$GrA^2\left[\frac{A}{\rho+Ax}J(\psi,\omega) + \left(\frac{A}{\rho+Ax}\right)^2\omega\frac{\partial\psi}{\partial z}\right] = -\frac{\partial\theta}{\partial x} + A\nabla_2^2\omega + A^2\left(\frac{1}{\rho+Ax}\frac{\partial\omega}{\partial x} - \frac{\omega}{(\rho+Ax)^2}\right) \tag{2}$$

$$\omega = -\frac{A}{\rho+Ax}\nabla_2^2\psi + \left(\frac{A}{\rho+Ax}\right)^2\frac{\partial\psi}{\partial x} \tag{3}$$

$$Gr\,Pr\frac{A^2}{\rho+Ax}J(\psi,\theta) = \nabla_2^2\theta + \frac{A}{\rho+Ax}\frac{\partial\theta}{\partial x} \tag{4}$$

$$\psi = \frac{\partial\psi}{\partial z} = \frac{\partial\theta}{\partial z} = 0 \quad \text{at } z = 0, 1 \tag{5a}$$

$$\psi = \frac{\partial\psi}{\partial z} = 0, \quad \theta = 1 - Ax \quad \text{at } x = 0, A^{-1}. \tag{5b}$$

Here,

$$x \equiv (r - r_h)/h$$

$$J(C,D) \equiv \frac{\partial C}{\partial x}\frac{\partial D}{\partial z} - \frac{\partial C}{\partial z}\frac{\partial D}{\partial x}$$

$$\nabla_2^2 \equiv \frac{\partial^2}{\partial x^2} + \frac{\partial^2}{\partial z^2}.$$

The dimensionless parameters which appear are

$Gr = \frac{gh^3}{\nu^2}\beta(T_h - T_c)$ (Grashof number)

$Pr = c_p\mu/k$ (Prandtl number)

$A = h/(r_c - r_h)$ (cavity aspect ratio)

$\rho = A\delta = r_h/(r_c - r_h)$ (annulus aspect ratio).

Comparison with the two-dimensional problem of [3] shows the presence of one additional parameter in the present case, namely the aspect ratio ρ (or, alternatively, $\delta \equiv r_h/h$).

We seek solutions of equations (2)–(5) for arbitrary, but fixed, values of Gr and Pr in the limit as the cavity becomes very shallow relative to its breadth, i.e. as $A \to 0$. There are two cases of interest for the geometric parameter ρ. In the first, the ratio of the radius r_h to the height h is held fixed, i.e. $\delta = O(1)$ so that $\rho \to 0$ as $A \to 0$. In the second, ρ is held fixed as $A \to 0$; thus $\delta \to \infty$. This second case includes the 2-D limit for $\rho \gg 1$. We shall see that the detailed analysis for the two limits, $\delta = O(1)$ and $\rho = O(1)$, is fundamentally different. It is therefore a surprise that the solutions in the core region are identical to the level of approximation of the present analysis.

Following Cormack *et al.* [3], we seek solutions of equations (2)–(4) which exhibit a parallel flow structure to at least a first level of approximation (i.e. to $O(1)$ in A). The boundary conditions (5b) at $x = 0$, A^{-1} show clearly that a solution of this type is only possible in the core of the cavity, away from the end-walls. Thus, the central core solution must be supplemented by separate solutions in the two end-regions, i.e. near $r = r_c$ and r_h, which match with the core solution in the usual asymptotic sense as $A \to 0$.

The governing equations (2)–(4) can be expressed in a form which is more appropriate for the core region by noting that a parallel flow structure must correspond to a characteristic length scale $(r_c - r_h)$ in the x-direction, rather than h as assumed in the nondimensionalization which led to equations (2)–(5). Thus, it is convenient to rescale the equations according to

$$\hat{x} = Ax \quad \text{and } \hat{\psi} = A\psi.$$

For ease in distinguishing core variables from those in the end-regions, we also use $\hat{\theta}$ and $\hat{\omega}$ in place of θ and ω. With these changes, the governing equations (2)–(4) can be re-expressed in a form suitable to the core-region.

$$Gr\,A^2\left[\frac{1}{\rho+\hat{x}}\hat{J}(\hat{\psi},\hat{\omega}) + \frac{\hat{\omega}}{(\rho+\hat{x})^2}\frac{\partial\hat{\psi}}{\partial z}\right] = -\frac{\partial\hat{\theta}}{\partial\hat{x}} + \frac{\partial^2\hat{\omega}}{\partial z^2} + A^2\left[\frac{\partial^2\hat{\omega}}{\partial\hat{x}^2} + \frac{1}{\rho+\hat{x}}\frac{\partial\hat{\omega}}{\partial\hat{x}} - \hat{\omega}(\rho+\hat{x})^2\right] \tag{6}$$

$$\hat{\omega} = -\frac{1}{\rho+\hat{x}}\frac{\partial^2\hat{\psi}}{\partial z^2} - \frac{A^2}{\rho+\hat{x}}\left(\frac{\partial^2\hat{\psi}}{\partial\hat{x}^2} - \frac{1}{\rho+\hat{x}}\frac{\partial\hat{\psi}}{\partial\hat{x}}\right) \tag{7}$$

$$Gr\,Pr\frac{A^2}{\rho+\hat{x}}\hat{J}(\hat{\psi},\hat{\theta}) = \frac{\partial^2\hat{\theta}}{\partial z^2} + A^2\left(\frac{\partial^2\hat{\theta}}{\partial\hat{x}^2} + \frac{1}{\rho+\hat{x}}\frac{\partial\hat{\theta}}{\partial\hat{x}}\right) \tag{8}$$

in which $\hat{x}$ and ρ are both $O(1)$. As written, these equations are suitable for the limiting problem, $A \to 0$, $\rho = O(1)$. To transform to a form appropriate to the case $A \to 0$, $\delta = O(1)$, we can introduce δ $(\equiv \rho/A)$ in place of ρ. However, at the level of approximation which we will consider, this is equivalent to simply putting $\rho = 0$ and solutions for both cases are thus obtainable directly from equations (6)–(8). The fundamental distinction between $\rho = O(1)$ and $\delta = O(1)$ does *not* appear in the governing equations for the core region. It is only in the vicinity of the end-walls that the difference between the two cases actually plays an important role in the governing equations. In the core region we thus seek solutions of equations (6)–(8) in the form of an asymptotic expansion

$$\{\hat{\theta}, \hat{\psi}, \hat{\omega}\} = \sum_{i=0}^{N} A^i \{\hat{\theta}_i, \hat{\psi}_i, \hat{\omega}_i\} \tag{9}$$

for both $\rho = O(1)$ and $\delta = O(1)$. The governing equations at $O(1)$, are just

$$\frac{\partial \hat{\theta}_0}{\partial \hat{x}} = \frac{\partial^2 \hat{\omega}_0}{\partial z^2} \tag{10a}$$

$$\hat{\omega}_0 = -\frac{1}{\rho + \hat{x}} \frac{\partial^2 \hat{\psi}_0}{\partial z^2} \tag{10b}$$

$$\frac{\partial^2 \hat{\theta}_0}{\partial z^2} = 0. \tag{10c}$$

Although the equations and boundary conditions in the core are independent of the choice $\rho = O(1)$ or $\delta = O(1)$, it is still possible that the solutions for these two cases may differ due to differences in the matching conditions with the end-region solutions.

In the end-regions, the characteristic length scale is $O(h)$ in both coordinate directions, as already assumed in equations (2)–(4). On the other hand, if a parallel flow structure exists in the core at $O(1)$, all streamlines must enter the end-regions, and it is clear that the scaling for horizontal velocity must be the same as in the core. Thus, introducing

$$\psi = A^{-1} \bar{\psi}$$

into equations (2)–(4), we obtain a form for the governing equations which is appropriate for the end-regions ($r \sim r_h$ and $r \sim r_c$)

$$Gr\, A^2 \left[\frac{1}{\rho + Ax} J(\bar{\psi}, \omega) + \frac{A\omega}{(\rho + Ax)^2} \frac{\partial \bar{\psi}}{\partial z} \right] = -\frac{\partial \theta}{\partial x} + A \nabla_2^2 \omega + \frac{A^2}{\rho + Ax} \frac{\partial \omega}{\partial x} - \frac{A^3 \omega}{(\rho + Ax)^2} \tag{11}$$

$$\omega = -\frac{1}{\rho + Ax} \nabla_2^2 \bar{\psi} + \frac{A}{(\rho + Ax)^2} \frac{\partial \bar{\psi}}{\partial x} \tag{12}$$

and

$$Gr\, Pr \frac{A}{\rho + Ax} J(\bar{\psi}, \theta) = \nabla_2^2 \theta + \frac{A}{\rho + Ax} \frac{\partial \theta}{\partial x}. \tag{13}$$

These equations are suitable for the case in which $A \to 0$ with $\rho = O(1)$. It will be noted that a considerable simplification takes place if this limit is applied directly to equations (11)–(13), and this is reflected by the simple governing equations which appear at each order in A when an asymptotic representation of the form

$$\{\theta, \bar{\psi}, \omega\} = \sum_{i=0}^{N} A^i \{\theta_i, \bar{\psi}_i, \omega_i\} \tag{14}$$

is adopted as required by the conditions of matching with equation (9). At $O(1)$, these equations are simply

$$\frac{\partial \theta_0}{\partial x} = 0; \quad \nabla_2^2 \theta_0 = 0. \tag{15}$$

In order to obtain a form of the governing equations (11)–(13) which is suitable for the limiting problem $A \to 0$ with $\delta = O(1)$, we introduce $\rho = A\delta$ and then note from (12) that $\omega = A^{-1}\bar{\omega}$ in order that $\bar{\omega} = O(1)$. It thus follows that

$$Gr \left[\frac{1}{x + \delta} J(\bar{\psi}, \bar{\omega}) + \frac{\bar{\omega}}{(x + \delta)^2} \frac{\partial \bar{\psi}}{\partial z} \right] = -\frac{\partial \theta}{\partial x} + \nabla_2^2 \bar{\omega} + \frac{1}{x + \delta} \frac{\partial \bar{\omega}}{\partial x} - \frac{\bar{\omega}}{(x + \delta)^2} \tag{16}$$

$$\bar{\omega} = \frac{1}{(x + \delta)} \nabla_2^2 \bar{\psi} + \frac{1}{(x + \delta)^2} \frac{\partial \bar{\psi}}{\partial x} \tag{17}$$

$$Gr\, Pr\, J(\bar{\psi}, \theta) = \nabla_2^2 \theta + \frac{1}{x + \delta} \frac{\partial \theta}{\partial x}. \tag{18}$$

Unlike the end-region equations (11)–(13) for $\rho = O(1)$, these equations for $\delta = O(1)$ are independent of A. Thus, in spite of the fact that the conditions for matching still suggest an expansion of the form

$$\{\theta, \bar{\psi}, \bar{\omega}\} = \sum_{i=0}^{N} A^i \{\theta_i, \bar{\psi}_i, \bar{\omega}_i\} \tag{19}$$

for $\delta = O(1)$, the governing equations at $O(1)$ appear to be the *full* nonlinear equations (16)–(18) rather than the very simple equations (15) which arose in the case $A \to 0$ ($\rho = O(1)$). Fortunately, when $\delta = O(1)$, the core solution provides a second small parameter $[\ln(\rho/1 + \rho)]^{-1}$ at each order in A and the end-region problem simplifies a great deal.

3. SOLUTION OF THE PROBLEM

We now turn to the solution of our problem for $A \to 0$ and either $\rho = O(1)$ or $\delta = O(1)$. In both cases, the core equations are (6)–(8) with the expansion (9) and $O(1)$ equations (10a)–(10c). The end-regions are governed by equations (11)–(13) and (15)–(18), respectively, with asymptotic expansions (14) and (19). The solutions in the core and end-regions must be matched according to

$$\lim_{\hat{x} \to 0} \{\hat{\theta}, \hat{\psi}, \hat{\omega}\}_{CORE} \Leftrightarrow \begin{cases} \lim_{x \to \infty} \{\theta, \bar{\psi}, \omega\}_{HOT\ END} \\ \text{or} \\ \lim_{x \to \infty} \{\theta, \bar{\psi}, \bar{\omega}\}_{HOT\ END} \end{cases} \text{as } A \to 0 \tag{20}$$

and

$$\lim_{\hat{x} \to 1} \{\hat{\theta}, \hat{\psi}, \hat{\omega}\}_{CORE} \Leftrightarrow \begin{cases} \lim_{\xi \to \infty} \{\theta, \bar{\psi}, \omega\}_{COLD\ END} \\ \text{or} \\ \lim_{\xi \to \infty} \{\theta, \bar{\psi}, \bar{\omega}\}_{COLD\ END} \end{cases} \text{as } A \to 0$$

with $\xi = A^{-1} - x$.

The solution scheme is similar, in some respects, to that of Cormack *et al.* [3] for the 2-D case. However, unlike the 2-D problem where a single solution was found to be valid at all orders in A for the core, the 3-D problem must be solved step-by-step in A for both the core and end-regions. In addition, in the present paper, we focus our attention on the Nusselt number which gives the overall rate of heat transport from the hot cylinder wall to the cold one, and thus adopt a solution scheme which does not require a full resolution of the end-region solutions. We begin with the core solution at $O(1)$ which is common to both problems $\delta = O(1)$ and $\rho = O(1)$. It is then necessary to examine higher-order core terms and solutions in the ends separately for these two cases.

(a) *Core solutions at* $O(1)$

The governing equations in the core at $O(1)$ are (10a)–(10c). Thus, starting with (10c), we can obtain the general solution form

$$\theta_0 = g_1(\hat{x};\rho)z + g_0(\hat{x};\rho) \qquad (21a)$$

$$\hat{\psi} = m(\hat{x};\rho) + n(\hat{x};\rho)z - \left(h(\hat{x};\rho)\frac{z^2}{2} + k(\hat{x};\rho)\frac{z^2}{6}\right)\hat{x} - \left(f'(\hat{x};\rho)\frac{z^4}{24} + g'(\hat{x};\rho)\frac{z^5}{120}\right)\hat{x} \qquad (21b)$$

and

$$\omega_0 = f'(\hat{x};\rho)\frac{z^2}{2} + g'(\hat{x};\rho)\frac{z^3}{6} + h(\hat{x};\rho) + k(\hat{x};\rho)z. \qquad (21c)$$

If we assume the flow to be parallel at this order in A, see also Fig. 1(b),

$$m, n = \text{constant};\ h = \frac{h_0}{\hat{x}},\ k = \frac{k_0}{\hat{x}},$$

$$f'(\hat{x}) = \frac{f_0}{\hat{x}},\ g'(x) = \frac{g_0}{\hat{x}}$$

with h_0, k_0, f_0, g_0 = constant. Thus, applying boundary conditions (5a) at $z = 0, 1$ we can show

$$\theta_0 = c_0 \ln(\hat{x} + \rho) + c_0^* \qquad (22a)$$

$$\hat{\psi}_0 = -c_0 F'(z) \qquad (22b)$$

$$\omega_0 = c_0 \frac{1}{\hat{x} + \rho} F'''(z) \qquad (22c)$$

where

$$F'(z) = \frac{z^4}{24} - \frac{z^3}{12} + \frac{z^2}{24}.$$

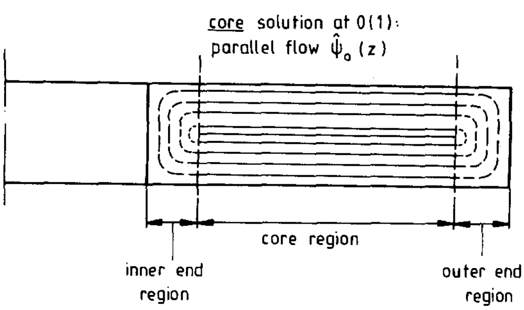

FIG. 1(b). Schematic diagram of the stream function at $O(1)$.

The constants c_0 and c_0^* must be obtained by matching with solutions in the end-regions.

(b) *Higher-order solution for* $A \to 0$, $\rho = O(1)$

To go further we must examine the end-flows and the higher-order corrections in the core separately for the two cases $\rho = O(1)$ and $\delta = O(1)$. Here we consider $\rho = O(1)$ where the first, $O(1)$, terms in end-regions are governed by equation (15). Seeking a solution for θ_0 in the ends as a simple power series expansion in x and z, and applying the boundary conditions (5b) on θ, we find only the trivial solutions at $O(1)$

$$\text{hot end:}\quad \theta_0^h = 1$$

$$\text{cold end:}\quad \theta_0^c = 0.$$

Following the matching principles (20) we thus find

$$c_0 \ln \rho + c_0\left[\frac{Ax}{\rho} - \frac{1}{2}\left(\frac{Ax}{\rho}\right)^2 + \ldots\right] + c_0^* = 1$$

(hot end)

$$c_0 \ln(1+\rho) + c_0\left[-\frac{A\xi}{1+\rho} - \frac{1}{2}\left(\frac{A\xi}{1+\rho}\right)^2 - \ldots\right] + c_0^* = 0 \text{ (cold end).}$$

The constants c_0 and c_0^* which satisfy these matching conditions to $O(1)$ are

$$c_0 = \frac{1}{\ln\left(\dfrac{\rho}{1+\rho}\right)} \quad\text{and}\quad c_0^* = -\frac{\ln(1+\rho)}{\ln\left(\dfrac{\rho}{1+\rho}\right)}. \qquad (24)$$

The mismatch remaining at $O(A)$, $O(A^2)$... must be taken into account when matching at higher orders in the approximation scheme.

At $O(A)$, the solution for θ_1 in the ends may be shown, in a similar fashion, to be of the simple form

$$\theta_1^h = \frac{c_0}{\rho} x \qquad \text{(hot end)}$$

$$\theta_1^c = -\frac{c_0}{1+\rho}\xi \qquad \text{(cold end),} \qquad (25)$$

while the core solution $(\hat{\theta}_1, \hat{\psi}_1, \hat{\omega}_1)$ is identically zero. Since our interest is mainly with the core flow and with the Nusselt number, we do not attempt to solve the equations for ω_0 and $\bar{\psi}_0$ which arise at $O(A)$ in the end-regions.

Finally, at $O(A^2)$ in the core we have the governing equations

$$\frac{\partial \theta_2}{\partial \hat{x}} = \frac{\partial^2 \omega_2}{\partial z^2} + 2c_0^2\, Gr \frac{F''(z)F'''(z)}{(\rho + \hat{x})^3} \qquad (26a)$$

$$\omega_2 = -\frac{1}{\rho + \hat{x}} \frac{\partial^2 \hat{\psi}_2}{\partial z^2} \qquad (26b)$$

$$\frac{\partial^2 \theta_2}{\partial z^2} = c_0^2\, Gr\, Pr \frac{F''(z)}{(\rho + \hat{x})^2}. \qquad (26c)$$

After some algebra, these yield general solutions which satisfy the boundary conditions at $z = 0, 1$.

$$\hat{\theta}_2 = f_2(\hat{x};\rho) + c_0^2\, Gr\, Pr \frac{F(z)}{(\rho + \hat{x})^2} \tag{27a}$$

$$\hat{\psi} = -(\hat{x} + \rho) f_2'(\hat{x};\rho) F'(z) + 2c_0^2\, Gr \frac{G(z) + PrH(z)}{(\rho + \hat{x})^2} \tag{27b}$$

$$\hat{\omega}_2 = f_2'(\hat{x};\rho) F'''(z) - 2c_0^2\, Gr \frac{G''(z) + PrH''(z)}{(\rho + \hat{x})^3} \tag{27c}$$

where*

$$F(z) = \frac{z^5}{120} - \frac{z^4}{48} + \frac{z^3}{72} - \frac{1}{1440} \tag{28a}$$

$$G(z) = \frac{1}{8!}\left(\frac{10}{9}z^9 - 5z^8 + \frac{26}{3}z^7 - 7z^6 + \frac{7}{3}z^5 - \frac{1}{9}z^3\right) \tag{28b}$$

$$H(z) = \frac{1}{8!}\left(\frac{1}{9}z^9 - \frac{1}{2}z^8 + \frac{2}{3}z^7 - \frac{7}{6}z^4 + \frac{11}{9}z^3 - \frac{1}{3}z^2\right). \tag{28c}$$

In contrast to the 2-D case, the core flow is *not* parallel at $O(A^2)$. Furthermore, the Prandtl number appears not only within the product $GrPr$, as it does in the 2-D case, but also has a more complicated influence in $\hat{\psi}_2$ and ω_2. The function $f_2(\hat{x}, \rho)$ must be obtained by matching the core- and end-flows at $O(A^2)$. Fortunately, this may be done quite simply without any need to solve explicitly for the temperature function θ_2 or the streamfunction/vorticity $\bar{\psi}_1, \omega_1$ in the ends. At $O(A^2)$, the matching condition on θ in the hot end is simply

$$-\frac{c_0 x^2}{2\rho^2} + f_2(\hat{x};\rho) + c_0^2\, Gr\, Pr \frac{F(z)}{(\rho + Ax)^2} \Leftrightarrow \theta_2^h \quad \text{as } A \to 0. \tag{29}$$

On the other hand, the governing equation for the end-region solution, θ_2^h, is

$$\frac{\partial^2 \theta_2^h}{\partial x^2} + \frac{\partial^2 \theta_2^h}{\partial z^2} = -\frac{1}{\rho + Ax}\frac{c_0}{\rho} - Gr\, Pr \frac{1}{\rho + Ax}\frac{c_0}{\rho}\frac{\partial \bar{\psi}_0}{\partial z}. \tag{30}$$

Integrating equation (30) with respect to z from $z = 0$ to $z = 1$ and applying the boundary conditions for θ_2^h and $\bar{\psi}_0$ at these points gives

$$\int_{z=0}^{1} \frac{\partial^2 \theta_2^h}{\partial x^2} dz = -\frac{c_0}{\rho}\frac{1}{\rho + Ax}. \tag{31}$$

Thus

$$\int_{z=0}^{1} \theta_2^h dz = -\frac{c_0}{\rho^2}\frac{\rho}{A}\left(\frac{A}{\rho}\frac{x^2}{2} - \frac{A^2}{\rho^2}\frac{x^3}{6} + \dots\right) + K_2 x \tag{32}$$

and substitution for θ_2^h from equation (29) gives

$$-\frac{c_0 x^2}{2\rho^2} + f_2(\hat{x};\rho) \Leftrightarrow -\frac{c_0}{\rho^2}\frac{x^2}{2} + \frac{A c_0}{6\rho^3}x^3 - \dots + K_2 x. \tag{33}$$

It follows that

$$f_2(\hat{x};\rho) = K_2 = 0 \tag{34}$$

and this completes the core flow solution to $O(A^2)$ for $A \to 0$ with ρ fixed.

(c) *Higher-order solutions for $A \to 0$, $\delta = O(1)$*

Let us now turn to the limit $A \to 0$ with $\delta = O(1)$. We have already noted that this case appears more difficult than the limit $A \to 0$, $\rho = O(1)$ because the governing equations at $O(1)$ in the end region do not obviously simplify when $A \to 0$. However, this apparent difficulty is easily overcome, and the problem can be reduced to a form which is comparable to that for $\rho = O(1)$. A simple motivation for this simplification follows from the observation that the *core* solution (22a) for $\hat{\theta}_0$ can satisfy the boundary-condition (5b) exactly at $x = 0, 1$. The result of putting $\hat{\theta}_0 = 1$ at $\hat{x} = 0$ is just

$$\hat{\theta}_0 = \frac{\ln\left(\dfrac{\rho + Ax}{1 + \rho}\right)}{\ln\left(\dfrac{\rho}{1 + \rho}\right)}. \tag{35}$$

There is, of course, no guarantee that the form obtained in this way will be the same as that obtained by proper matching with solutions in the end-domains. However, this was shown to be true in the preceding case [cf. equations (24)] and will also be demonstrated in this section for $A \to 0$, $\delta = O(1)$.

Assuming equation (35) to be correct for the moment, the solution scheme in this second case is easily motivated. In particular, though $\hat{\theta}_0$ is clearly $O(1)$ for $A \to 0$, $\rho = O(1)$, the combination $\varepsilon = \{\ln[\rho/(1 + \rho)]\}^{-1}$ is asymptotically small in the limit $A \to 0$ with $\delta = O(1)$.†

Anticipating the requirements for matching with the end-region solutions, this suggests the use of a double expansion of the form

$$\bar{\theta} = \bar{\theta}_0^0 + \sum_{i=0}^{\infty} A^i\left[\sum_{k=1}^{\infty}\left(\frac{1}{\ln\dfrac{\rho}{1+\rho}}\right)^k \bar{\theta}_i^k\right] \tag{36a}$$

$$(\bar{\psi}, \bar{\omega}) = \sum_{i=0}^{\infty} A^i\left[\sum_{k=1}^{\infty}\left(\frac{1}{\ln\dfrac{\rho}{1+\rho}}\right)^k (\bar{\psi}_i^k, \bar{\omega}_i^k)\right] \tag{36b}$$

*Note, $8! = 1 \times 2 \times 3 \times \dots 7 \times 8 = 40320$.

†Note, $\rho \to 0$ as $A \to 0$ if $\delta = O(1)$.

in place of equation (19). A similar form is then also required in the core

$$(\hat{\theta},\bar{\psi},\bar{\omega}) = \sum_{i=0}^{\infty} A^i\left[\sum_{k=1}^{\infty}\left(\frac{1}{\ln\dfrac{\rho}{1+\rho}}\right)^k(\hat{\theta}_i^k,\hat{\psi}_i^k,\hat{\omega}_i^k)\right]. \tag{37}$$

With the expansion (36), we see from equations (16)–(18) that

$$\frac{\partial\bar{\theta}_0^0}{\partial x} = 0, \quad \nabla^2\theta_0^0 = 0$$

in the end-regions, and thus

$$\begin{aligned} \bar{\theta}_0^0|_h &= 1 \qquad \text{(hot end)} \\ \bar{\theta}_0^0|_c &= 0 \qquad \text{(cold end)} \end{aligned} \tag{38}$$

as before. The result of matching equations (38) and (22a) is the expression (35) for the term at $i = 0$, $k = 1$ in equation (31), and the corresponding solution in the core, i.e. $(\hat{\theta}_0^1, \hat{\psi}_0^1, \hat{\omega}_0^1)$, is precisely equation (22) with c_0, c_0^* given by equation (24). Thus, at first-order, there is no difference between the solutions for $A \to 0$ with $\rho = O(1)$, and $A \to 0$ with $\delta = O(1)$.

The mismatch between equation (35) and $\hat{\theta}_0'$ [i.e. (35)] is remedied at $k = 1$ in the expansion for $(\bar{\theta}_0, \bar{\psi}_0, \bar{\omega}_0)$. Substituting equation (36) into equations (16)–(18) and equating terms of equal order in $\{\ln[\rho/(1+\rho)]\}^{-1}$ for $i = 0$, we find

$$\nabla^2\bar{\theta}_0^1 = 0 \tag{39a}$$

$$\frac{\partial\bar{\theta}_0^1}{\partial x} = \nabla^2\bar{\omega}_0^1 - \frac{\bar{\omega}_0^1}{(x+\delta)^2} \tag{39b}$$

$$\nabla^2\bar{\psi}_0^1 - \frac{2}{x+\delta}\frac{\partial\bar{\psi}_0^1}{\partial x} = -(x+\delta)\bar{\omega}_0^1. \tag{39c}$$

A general solution of equation (39a) can be obtained by standard methods

$$\bar{\theta}_0^1 = c\ln(x+\delta) + d + \sum_{n=1}^{\infty} A_n F_n(x)\cos(n\pi z)$$

which satisfies boundary conditions at $z = 0, 1$. The boundary conditions at $x = 0$ and $x = A^{-1}$ plus matching with $\hat{\theta}_0^1\{\ln[\rho/(1+\rho)]\}^{-1}$, then yields

$$\left[\bar{\theta}_0^0 + \frac{1}{\ln\left(\dfrac{\rho}{1+\rho}\right)}\bar{\theta}_0^1\right]\Bigg|_h = 1 - \frac{\ln\left(\dfrac{Ax+\rho}{\rho}\right)}{\ln\left(\dfrac{1+\rho}{\rho}\right)} \qquad \text{(hot end)} \tag{40}$$

and

$$\left[\bar{\theta}_0^0 + \frac{1}{\ln\left(\dfrac{\rho}{1+\rho}\right)}\bar{\theta}_0^1\right]\Bigg|_c = \frac{\ln\left(\dfrac{Ax+\rho}{1+\rho}\right)}{\ln\left(\dfrac{\rho}{1+\rho}\right)} \qquad \text{(cold end).} \tag{41}$$

The match between $\hat{\theta}_0^1$ and these end-solutions equations (40) and (41) is *exact*.

The governing equations for the fluid motion $(\bar{\psi}_0^1, \bar{\omega}_0^1)$ are obtained by substitution of equations (40) and (41) into (39b, c), i.e.

$$\begin{aligned} \nabla^2\bar{\omega}_0^1 - \frac{\bar{\omega}_0^1}{(x+\delta)^2} &= +\frac{1}{x+\delta}; \\ \nabla^2\bar{\psi}_0^1 - \frac{2}{x+\delta}\frac{\partial\bar{\psi}_0^1}{\partial x} &= -(x+\delta)\bar{\omega}_0^1. \end{aligned} \tag{42}$$

These non-homogeneous equations are to be solved subject to the boundary conditions

$$\begin{aligned} \bar{\psi}_0^1 = \frac{\partial\bar{\psi}_0^1}{\partial z} &= 0 \qquad z = 0, 1 \\ \bar{\psi}_0^1 = \frac{\partial\bar{\psi}_0^1}{\partial x} &= 0 \qquad x = 0 \end{aligned} \tag{43}$$

plus matching with $(\hat{\psi}_0^1, \hat{\omega}_0^1)\,\{\ln[\rho/(1+\rho)]\}^{-1}$, e.g.

$$\begin{aligned} \lim_{x\to\infty}\bar{\psi}_0^1 &\to -\left(\frac{z^4}{24} - \frac{z^3}{12} + \frac{z^2}{24}\right) \\ \lim_{x\to\infty}\frac{\partial\bar{\psi}_0^1}{\partial x} &\to 0. \end{aligned} \tag{44}$$

Although a closed-form analytic solution may be obtained for equations (42)–(44), we do not display it here as it is not essential to the analysis which follows.

Higher order solutions will also exist for $i = 0$ in the end regions owing to the fact that $\partial\bar{\psi}_0^1/\partial z$ is nonzero. Indeed, the velocity field corresponding to $\bar{\psi}_0^1$ acts as a convective 'source' in the governing differential equation for $\bar{\theta}_0^2$, while $\bar{\theta}_0^2$ drives the flow associated with $\bar{\psi}_0^2$. In turn $\bar{\psi}_0^2$ yields $\bar{\theta}_0^3$ and so on for larger values of k. We shall explicitly consider only $\bar{\theta}_0^2$ which represents the first direct contribution of convection in the end-regions. The governing differential equation for $\bar{\theta}_0^2$ can be obtained from equation (18) and is

$$\nabla^2\bar{\theta}_0^2 = -\frac{Gr\,Pr}{x+\delta}\frac{\partial\bar{\psi}_0^1}{\partial z} \tag{45}$$

with homogeneous boundary conditions

$$\begin{aligned} \bar{\theta}_0^2 &= 0 \qquad x = 0 \\ \frac{\partial\bar{\theta}_0^2}{\partial z} &= 0 \qquad z = 0, 1 \end{aligned}$$

and matching with the core solution. We have noted that the term on the right hand side of equation (45) is due to thermal convection. It may, at first, seem surprising that a convection contribution should arise in the end region at $O(1)$, with respect to A, when the first contribution of convection in the *core* will only appear at $O(A^2)$ [cf. equations (6–8)]. However, we shall see that there is an exact match between $\bar{\theta}_0^2$ and this first convection term in the core. To demonstrate this fact, we will not require a complete solution for $\bar{\theta}_0^2$; only its asymptotic form for large x. This may be obtained very easily by making use of the asymptotic form for $\bar{\psi}_0^1$ from the matching condition (44) for large x. This yields the differential equation

$$\nabla^2 \bar{\theta}_0^2 \sim \frac{Gr\,Pr}{(x+\delta)^2}\left(\frac{z^3}{6}-\frac{z^2}{4}+\frac{z}{12}\right)$$

for $x \gg 1$, and it follows that

$$\bar{\theta}_0^2 \sim \frac{Gr\,Pr}{(x+\delta)^2}\left(\frac{z^5}{120}-\frac{z^4}{48}+\frac{z^3}{72}-\frac{1}{1440}\right); \qquad (x \gg 1). \quad (46)$$

Transforming to the core variables $\hat{x}$ and ρ, this becomes

$$\bar{\theta}_0^2 \sim A^2\frac{Gr\,Pr}{(\hat{x}+\rho)^2}\left(\frac{z^5}{120}-\frac{z^4}{48}+\frac{z^3}{72}-\frac{1}{1440}\right) \quad (47)$$

and the mismatch with $\hat{\theta}_0$ is seen to be $O\{A^2/[\ln(\rho/1+\rho)]^2\}$. Although the higher-order terms, $\bar{\theta}_0^3, \bar{\theta}_0^4 \ldots$ yield a further mismatch with the core solution $\hat{\theta}_0$, it is of smaller magnitude, $O\{A^2/[\ln(\rho/1+\rho)]^2\}$, and we shall not consider these terms here.

Turning now to the core region, we have so far only discussed the terms $\hat{\theta}_0^1$, $\hat{\psi}_0^1$ and $\hat{\omega}_0^1$. The differential equations and boundary conditions for $i = 0$ and $k \geq 2$ and for $i = 1$ with $k \geq 1$ are all homogeneous and it thus follows that any nonzero solutions for these values of i and k would have to be generated through a mismatch at $O(1)$ or $O(A)$ between $\hat{\theta}_0$, $\hat{\psi}_0$ or $\hat{\omega}_0$ and the solutions in the end-regions. In view of the fact that no such mismatch exists, it follows that

$$\hat{\theta}_0^k = 0 \qquad k \geq 2$$
$$\hat{\theta}_1^k = 0 \qquad k \geq 1. \quad (48)$$

The first nonzero correction to ($\hat{\theta}_0$, $\hat{\psi}_0$ and $\hat{\omega}_0$) thus arises at $O(A^2)$ with $k = 2$, and is due to the appearance of nonzero convection terms in the governing equations. Since the core solution is identical to that of the preceding section through terms of $O(1)$ in A, the relevant solution is just equation (21). This must be matched with the end solution for large x, equation (41), to obtain f_2. The result is

$$f_2 = 0,$$

which is identical to that previously obtained for the case $A \to 0$ with $\rho = O(1)$.

Thus, we have shown that the solution in the core region through terms of $O\{A^2/[\ln(\rho/1+\rho)]^2\}$ is identical for the two limiting cases $A \to 0$ with $\rho = O(1)$ and $A \to 0$ with $\delta = O(1)$. In view of the differences in the end regions [cf. equations (9)–(11) and (15)–(17)] this seems to us to be a rather unexpected result.

4. DISCUSSION AND DETERMINATION OF THE NUSSELT NUMBER

We have seen that the core solution, through terms of $O\{A^2/[\ln(\rho/1+\rho)]^2\}$, is identical for the two limits $A \to 0, \rho = O(1)$ and $A \to 0, \delta = O(1)$. The temperature distribution and streamfunction are

$$\hat{\theta} = \frac{\ln\left(\dfrac{\rho + Ax}{\rho+1}\right)}{\ln\left(\dfrac{\rho}{\rho+1}\right)} + \frac{Gr\,Pr\,A^2}{\ln\left(\dfrac{\rho}{\rho+1}\right)^2}\frac{F(z)}{(\rho+Ax)^2} + O\left\{\frac{A^2}{\ln\left(\dfrac{\rho}{1+\rho}\right)^2}\right\} \quad (49)$$

and

$$\hat{\psi} = -\frac{F'(z)}{\ln\left(\dfrac{\rho}{\rho+1}\right)} + \frac{2Gr\,A^2}{\ln\left(\dfrac{\rho}{\rho+1}\right)^2}\frac{G(z)+Pr\,H(z)}{(\rho+Ax)^2} + O\left\{\frac{A^2}{\ln\left(\dfrac{\rho}{1+\rho}\right)^2}\right\}. \quad (50)$$

The corresponding velocity components are

$$u(\hat{x},z) = \frac{1}{\rho+Ax}\frac{F''(z)}{\ln\left(\dfrac{\rho}{\rho+1}\right)} - \frac{2Gr\,A^2}{\ln\left(\dfrac{\rho}{\rho+1}\right)^2}\frac{G'(z)+Pr\,H'(z)}{(\rho+Ax)^2} + \ldots \quad (51a)$$

and

$$w(\hat{x},z) = -\frac{2Gr\,A^2}{\ln\left(\dfrac{\rho}{\rho+1}\right)^2}\frac{G(z)+Pr\,H(z)}{(\rho+Ax)^4} + \ldots \quad (51b)$$

The first term in equation (49) is the temperature profile due to heat conduction, whereas the second term is the first contribution from heat transport by convection. The form of the solution for $\hat{\theta}$ is similar to that found by Cormack *et al.* [3] for the 2-D case; in particular, the z dependence of the convection term is identical. However, there is an additional dependence of the convection term on lateral position, x, which did not appear in the 2-D case. More striking are the changes in the velocity field. It may be seen from either equation (50) or equation (51) that the core motion is only unidirectional at the first approximation, and this contrasts sharply with the 2-D case where the core motion was *unidirectional and preserved in form* at all levels of approximation. Furthermore, the z-dependence of the convection term in equation (51a) depends on Pr, and this also represents a change from the 2-D problem. In particular, the convection contribution in the present case is asymmetric in z by an amount which depends on Pr. The function $F(z)$ [and $F''(z)$], see Fig. 2, which contributes to $\hat{\theta}$ at $O(A^2)$ and u at $O(1)$ is identical to the function which plays the same role in the 2-D theory. The functions $G(z)$ and $H(z)$ which appear in the velocity component, w, are plotted

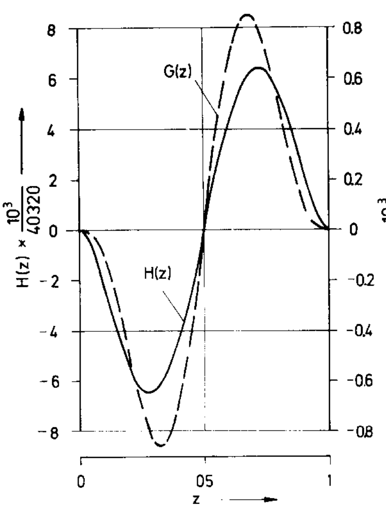

FIG. 2. Velocity profile $F''(z)$ at $O(1)$ and correction $F(z)$ to the temperature profile at $O(A^2)$.

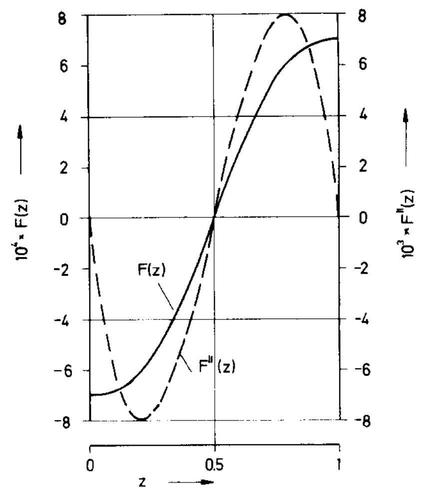

FIG. 3. Corrections $G(z)$ and $H(z)$ to the stream function $\hat{\psi}$ and to the velocity profile $\hat{w}$ at $O(A^2)$.

in Fig. 3. As noted above, these functions are not strictly symmetrical about $z = \frac{1}{2}$. Figure 4 shows the corresponding corrections $G'(z)$ and $H'(z)$ to the velocity component u at $O(A^2)$. In Fig. 5, the composite profiles $G(z) + Pr\,H(z)$ and $G'(z) + Pr\,H'(z)$ which appear in w and u, respectively, are plotted for $Pr = 7$.

The solutions (49) and (50) can be used to calculate the Nusselt number relating to the total heat flux due to conduction and convection between the two cylinders of the annular domain

$$Nu = \frac{\dot{Q}}{2\pi\lambda r_h(T_h - T_c)} \tag{52}$$

where, in dimensionless form,

$$\dot{Q} = 2\pi\lambda h(T_h - T_c)$$

$$\times \int_{z=0}^{z=1} \left[-(\rho + \hat{x})\frac{\partial\hat{\theta}}{\partial\hat{x}} + Gr\,Pr\,\hat{\psi}\frac{\partial\hat{\theta}}{\partial z} \right] dz. \tag{53}$$

Note, that $\dot{Q}$ is independent of $\hat{x}$ since the top and bottom of the cavity have been assumed to be insulated. Substituting for $\hat{\theta}$ and $\hat{\psi}$ from equations (49) and (50), we see that Nu can be calculated to $O(A^3)$ with the information available. A convection correction at $O(A^5)$, due to the $O(A^2)$ term in $\hat{\psi}$ can also be obtained, but is incomplete since higher order corrections are not known for $\hat{\theta}$. Thus, to $O(A^3)$ we obtain

$$Nu = \frac{A}{\rho \ln\left(\dfrac{1+\rho}{\rho}\right)} \times \left\{ 1 + 2.76 \times 10^{-6} \frac{(Gr\,Pr\,A)^2}{\rho \ln\left(\dfrac{1+\rho}{\rho}\right)^2} + O(A^3) \right\} \tag{54}$$

where

$$2.76 \times 10^{-6} \equiv \int_{z=0}^{z-1} [F'(z)]^2\,dz.$$

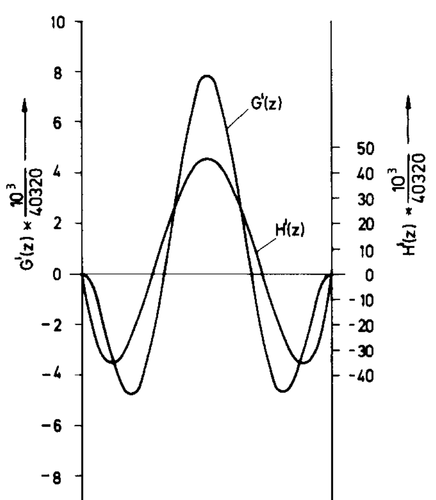

FIG. 4. Corrections $D'(z)$ and $H'(z)$ to the velocity profile $\hat{u}$ at $O(A^2)$.

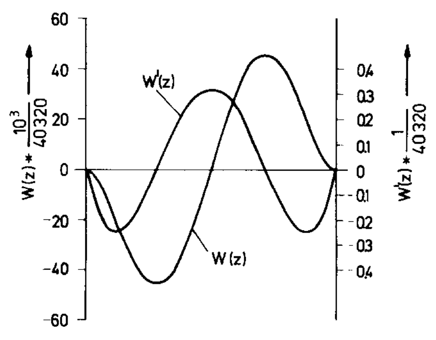

FIG. 5. Corrections $W'(z) = G'(z) + Pr\,H'(z)$ and $W(z) = G(z) + Pr\,H(z)$ to the velocity profiles $\hat{u}(z)$ and $\hat{w}(z)$, respectively at $O(A^2)$ where the Prandtl number is $Pr = 7$.

For r_c fixed and $r_h \to r_c$ for $A \ll 1$, the 3-D cavity reduces to the 2-D cavity and it is therefore of interest to calculate the limiting form for Nu. This follows simply from equation (54) by noting that

$$\lim_{\rho \to \infty} \left[\frac{1}{\rho \ln\left(\frac{1+\rho}{\rho}\right)} \right] \equiv 1.$$

The result is

$$Nu\,|_{\rho \to \infty} \to A[1 + 2.76 \times 10^{-6} (Gr\,Pr\,A)^2 + \dots].$$

This is identical to the result given by Cormack *et al.*[3, 5], with the exception of the constant 2.76×10^{-6} which was mistakenly reported as 2.86×10^{-6} in the previous analysis.

In the opposite limit r_c is fixed and $r_h \to 0$, i.e. $\rho \to 0$, the Nusselt number $Nu \to \infty$ for fixed A. This can easily be seen by using an approximation for the logarithm function

$$\frac{1}{\rho \ln\left(\frac{1+\rho}{\rho}\right)} \sim 0.22 \left(\frac{1}{\rho}\right)^{0.9245} \quad \text{as } \rho \to 0.$$

With the temperature difference fixed at $T_h - T_c$, the Nusselt number must become very large in order to maintain a finite heat flux when the surface area of the inner cylinder goes to zero.

Acknowledgements— Part of this work was done when one of the authors (G.P.M.) spent a year at the Department of Chemical Engineering at Caltech. He wishes to thank Professor Seinfeld and his colleagues for the warm hospitality he received and the DAAD for a NATO grant which made this stay possible.

REFERENCES

1. J. E. Hart, Stability of the flow in a differentially heated inclined box, *J. Fluid Mech.* **47**, 547–576 (1971).
2. D. E. Cormack, G. P. Stone and L. G. Leal, The effect of upper surface conditions on convection in a shallow cavity with differentially heated end-walls, *Int. J. Heat Mass Transfer* **18**, 635–648 (1975).
3. D. E. Cormack, L. G. Leal and J. Imberger, Natural convection in a shallow cavity with differentially heated end-walls — Part 1. Asymptotic theory, *J. Fluid Mech.* **65**, 209–229 (1974).
4. J. Imberger, Natural convection in a shallow cavity with differentially heated end-walls — Part 3. Experimental results, *J. Fluid Mech.* **65**, 247–260 (1974).
5. D. E. Cormack, L. G. Leal and J. H. Seinfeld, Natural convection in a shallow cavity with differentially heated end-walls — Part 2. Numerical solutions, *J. Fluid Mech.* **65**, 231–246 (1974).

CONVECTION NATURELLE DANS UNE CAVITE ANNULAIRE PEU PROFONDE

Résumé—On considère le problème de la convection naturelle dans une cavité annulaire et peu profonde avec des parois interne et externe différemment chauffées. Par rapport au problème bidimensionnel de Cormack, Leal et Imberger (1974), la structure de l'écoulement diffère de deux façons importantes. D'abord le coeur de l'écoulement est seulement parallèle à $O(1)$ dans l'anneau. Ensuite, le rayon fini du cylindre intérieur fournit une troisième échelle de longueur en plus de h et $(r_c - r_h)$. L'écoulement correspond à deux régimes distincts à la limite asymptotique $A = h/(r_c - r_h) \to 0$. La solution dans le coeur est développée à $O(A^2)$ et les résultats asymptotiques sont obtenus à $O(A^3)$ pour le nombre de Nusselt.

FREIE KONVEKTION IN EINEM FLACHEN RINGFÖRMIGEN HOHLRAUM

Zusammenfassung—Das Problem der freien Konvektion in einem flachen, ringförmigen Hohlraum mit unterschiedlich erwärmten inneren und äußeren Wänden wird betrachtet. Verglichen mit dem zweidimensionalen Problem bei Cormack, Leal und Imberger [3], weicht der Strömungsverlauf in zwei Punkten bedeutend ab. Erstens ist die Strömung im Kerngebiet des Ringraums nur von 1. Ordnung parallel. Zweitens stellt der endliche Radius des inneren Zylinders neben h und $(r_c - r_h)$ einen dritten Längenmaßstabsfaktor dar. Deshalb bestehen für die Strömung zwei Bereiche mit dem asymptotischen Grenzwert $A = h/(r_c - r_h) \to 0$. Die Lösung für das Kerngebiet wird korrekt von Ordnung (A^2) entwickelt, und für die Nusselt-Zahl erhält man asymptotische Ergebnisse, die bis Ordnung (A^3) gültig sind.

ЕСТЕСТВЕННАЯ КОНВЕКЦИЯ В УЗКОМ КОЛЬЦЕВОМ ЗАЗОРЕ

Аннотация — Исследуется естественная конвекция в узком кольцевом зазоре при наличии разности температур между внутренней и внешней стенками. Структура потока имеет две отличительные особенности по сравнению с двумерной задачей Кормака, Лиля и Имбергера (1974 г.). Во-первых, ядро потока параллельно только при $O(1)$ в кольцеобразном слое. И во-вторых, помимо h и $(r_c - r_h)$ имеется третий масштаб длины, представленный конечным радиусом внутреннего цилиндра. Поэтому в асимптотическом пределе $A = h/(r_c - r_h) \to 0$ можно четко выделить два режима. Решение для ядра справедливо вплоть до $O(A^2)$, а асимптотические значения, полученные для числа Нуссельта, справедливы вплоть до $O(A^3)$.